Thermally induced gluten modification observed with rheology and spectroscopies☆

Monika C. Wehrli [a], Tim Kratky [b], Marina Schopf [c], Katharina A. Scherf [c,d], Thomas Becker [a], Mario Jekle [a,*]

[a] Technical University of Munich, Chair of Brewing and Beverage Technology, Research Group Cereal Technology and Process Engineering, Weihenstephaner Steig 20, 85354 Freising, Germany
[b] Technical University of Munich, Department of Chemistry, Associate Professorship of Physical Chemistry with Focus on Catalysis, Lichtenbergstr, 4, 85748 Garching, Germany
[c] Leibniz-Institute for Food Systems Biology at the Technical University of Munich, Lise-Meitner-Str.34, 85354 Freising, Germany
[d] Karlsruhe Institute of Technology, Department of Bioactive and Functional Food Chemistry, Institute of Applied Biosciences, Adenauerring 20a, 76131 Karlsruhe, Germany

ARTICLE INFO

ABSTRACT

The protein vital gluten is mainly used for food while interest for non-food applications, like biodegradable materials, increases. In general, the structure and functionality of proteins is highly dependent on thermal treatments during production or modification. This study presents conformational changes and corresponding rheological effects of vital wheat gluten depending on temperature. Dry samples analyzed by X-ray photoelectron spectroscopy (XPS), Fourier-transform infrared spectroscopy (FTIR) and thermalgravimetric analysis coupled with mass spectrometry (TGA-MS) show surface compositions and conformational changes from 25 to 250 °C. Above 170 °C, XPS reveals a decreased N content at the surface while FTIR band characteristics for β-sheets prove structural changes. At 250 °C, protein denaturation accompanied by a significant mass loss due to dehydration and decarbonylation reactions is observed. Oscillatory measurements of optimally hydrated vital gluten describing network properties of the material show two structural changes along a temperature ramp from 25 to 90 °C: at 56–64 °C, the temperature necessary to trigger structural changes increases with the ratio of gliadin to total protein mass, determined by reversed-phase high performance liquid chromatography (RP-HPLC). At a temperature of 79–81 °C, complete protein denaturation occurs. FTIR confirms the denaturation process by showing band shifts with both temperature steps.

1. Introduction

As a by-product of the industrial wheat starch production, gluten increasingly gains importance for the use in a wide range of materials both for food and non-food applications [1,2]. The characteristics of dried and ground gluten, called vital gluten, are affected by the processing conditions as well as the constituents of the raw material [3] and are crucial for the quality of further products made from the protein [4–7]. While being processed the protein is subjected to various temperatures. As heat influences protein structures on a molecular level, such process steps alter the gluten network functionality [8–11]. This change in functionality can be characterized by the glass transition temperature (T_g) of gluten measured with differential scanning calorimetry (DSC). Transition temperatures of pure vital gluten powders are measured in the range of 155–164 °C [12]. Calculations considering the amino acid sequence reveal T_g values of 175 °C for glutenin and 186 °C for gliadin

[13]. In contrast, for hydrated gluten significantly lower T_g values in the range of 40.9–60.3 °C are found with augmenting water content (12.7–52.1%) [14]. Meanwhile Hoseney et al. (1986) determines T_g values of 50 °C for commercial and 38 °C for laboratory-isolated wet gluten [15]. This indicates that the denaturation and differences in protein functionality not only depend on the water content but also on the gluten composition. Wheat gluten can be subdivided in the two protein fractions gliadin and glutenin according to their solubility in aqueous alcohols. Gliadin can further be divided in ω5-, ω1,2-, α/β- and γ-gliadins [16]. Glutenin linked by interchain disulfide bonds can be split into low molecular weight (LMW) and high molecular weight (HMW) glutenins, with a size of 28–55 kDa and over 80 kDa, respectively [16–18]. The T_g of gluten changes with the amount of water and the gliadin to glutenin ratio [19] and can be further influenced by adding components such as sugars or lipids [20,21].

When implementing the protein into a hydrated system, the gliadin to glutenin ratio does not only influence T_g but decisively influences structural and thus rheological properties of the gluten matrix properties; the glutenin polymer is mainly responsible for the elastic behavior while the gliadin polymer significantly contributes to the viscous component [22]. Consequently, there is a visible rheological effect upon heating as well. Bale et al. (1970) states that heat denaturation shows

heat denaturation proportional to the temperature and an increasing number of cross links with no viscous deformation above 90 °C [11]. This means that at this temperature no rheological change can be detected. More specifically, hydrating pure vital gluten significantly varies the degree of conformational changes the material undergoes during heating. Heating gluten with a moisture content of 20–25% already reveals a clear decrease in both extensibility of the protein and glutenin extractability and results in less free sulphydryl groups [23,24]. Above 50 °C, the network is measurably affected; interpolypeptide disulphide bonds form between exposed groups of unfolded glutenins and the number of cross-links increases [11]. This effect was also pointed out by Georget et al. (2006) using Fourier-transform infrared spectroscopy (FTIR); their study additionally indicates that a loss of α-structures goes hand in hand with an irreversible formation of β-sheets that are then locked in by the formation of disulfide linkages [25]. FTIR has been proven to be an adequate method to analyze the structure of gluten and gluten subunits [26–28] as well as the interactions of single components within the material down to a molecular level [29,30]. However, FTIR studies on the structural alteration of proteins have not been linked to rheological data so far. Moreover, a direct link between thermally induced structural changes has never been directly drawn to other surface-sensitive measurements. A new possibility to investigate vital gluten in the absence of oxygen is presented by X-ray photoelectron spectroscopy (XPS) [31,32]. This technique can precisely determine the composition of a material surface such as the gluten matrix and the functional groups present at the surface at any temperature suitable for organic materials.

By analyzing structural changes with FTIR, XPS, thermalgravimetric analysis coupled with mass spectrometry (TGA-MS) and rheological methods thermally induced protein modifications are proven in both hydrated and dry vital gluten. An elaborate characterization of the thermal behavior contributes to a deeper understanding of gluten not only as a food product [33] but also as a renewable and biodegradable material in the non-food sector [1,2,34,35], like sustainable substitutes for plastic foils and containers. This is why the characteristics of vital gluten have already been determined both in combination with other materials [36–38] and in its pure form [23]. This knowledge can ultimately be used to tailor material properties by customizing parameters, such as temperature or hydration, during production processes. Based on the hypothesis, that structural changes are dependent on the interplay between temperature and hydration, this paper characterizes different technical vital gluten samples by exploiting their properties in dry and hydrated form. Hydrated gluten was measured only in a range from 20 to 95 °C to prevent evaporation of water during measurement. As the heat stability of dry gluten is higher, a temperature range of 20 to 250 °C was chosen to conduct experiments on gluten powder. In this paper, a surface-sensitive spectroscopy is combined with rheological measurements to characterize conformational changes in the material and directly correlate them with the mechanical response of thermal degradation. The experiments aim to investigate the behavior of the material during processing and its transformation for a wider range of use, such as packaging or medical materials.

2. Materials and methods

2.1. Materials

Vital wheat gluten from five different industrial suppliers (A-E) was used. All the analyses were done in triplicate and the values are based on dry mass displaying the mean ($n = 3$) and standard deviation.

Starch content (total starch enzyme kit by Megazyme International Ireland, Ltd., Wicklow, Ireland), fat content (Soxhlet measurement), ash content (ICC 104/1) and water retention capacity of the samples (AACC 56-11) are summarized in Table 1. The water absorption of the vital gluten samples was measured in a complex matrix made of 40% vital gluten and 60% glass beads (OMICRON NP5-P0, Microperl Sovitec,

Table 1
Basic analysis of the five vital gluten samples, including starch, fat and ash content and water retention capacity. All values come from measurements in triplicate and the mean and standard deviation were calculated.

Sample	Starch content [%]	Fat content [%]	Ash content [%]	Water retention capacity [%]
A	4.4 ± 0.7	1.11 ± 0.01	0.69 ± 0.01	151.4 ± 3.4
B	4.7 ± 0.9	1.17 ± 0.05	0.97 ± 0.00	150.2 ± 1.1
C	7.3 ± 0.7	1.51 ± 0.07	0.95 ± 0.01	153.3 ± 0.2
D	4.5 ± 0.4	1.08 ± 0.01	1.02 ± 0.01	149.8 ± 0.6
E	3.6 ± 0.1	1.72 ± 0.02	0.94 ± 0.01	162.6 ± 0.9

Schönborn, Germany) with a particle size of 2.60 μm to 19.27 μm acting as an inert filler [39] assuming no water absorption from the glass beads. This complex system has been chosen because the water absorption measurement of pure gluten in a z-kneading system (doughLAB, Perten Instruments, Hamburg, Germany) at 30 °C leads to inhomogeneous samples. After 8 min kneading time all samples showed a stable network indicated by a stable torque of the twin-screw at 550 ± 20 FU. The corresponding water absorption was measured and then calculated for 100% gluten samples assuming no water absorption from the glass beads.

3. Methods

3.1. Sample preparation

For Fourier-transform infrared spectroscopy (FTIR) and rheological measurements, a homogeneous network purely from vital gluten was developed by using a food processor (CH 6280 W, Grundig Intermedia GmbH, Fürth, Germany). Vital gluten powder was mixed in the device with its corresponding amount of water previously determined in the doughLAB for 60s so that a homogeneous sample is achieved. The preparation of hydrated gluten was repeated for every measurement.

3.2. Thermalgravimetric analysis coupled with mass spectrometry (TGA-MS)

Thermal gravimetric analysis was performed on a Netzsch STA 409 thermobalance (Netzsch-Gerätebau GmbH, Selb, Germany) connected to an Omnistar GSD 301 quadrupole mass spectrometer (Pfeiffer Vacuum Technology AG, Aßlar, Germany). The dry sample was heated in stream of 60 sccm 10% O_2/Ar. The temperature was linearly raised to 600 °C at a heating rate of 1 °C/min. The change of slope in the curve of the mass percentage was determined by the 1st derivative of the curve after binomial smoothing (one pass).

3.3. X-ray photoelectron spectroscopy (XPS)

X-ray photoelectron spectra were recorded on a Leybold-Heraeus LHS 10 spectrometer (Leybold, Cologne, Germany) using a non-monochromatized Mg Kα source (1253.6 eV). The powder samples were pressed into cavities and measured as pellets.

The analyzer was operated at a constant pass energy of 100 eV leading to an energy resolution with a full width at half-maximum (fwhm) of ~1.1 eV. The energy scale of the spectra was corrected for sample charging by using the C 1s main signal (285.0 eV). The denaturation of protein structures upon irradiation with X-rays was excluded by time-dependent measurements (see supporting information). All spectra were recorded in an ultra-high vacuum chamber at a pressure below 5×10^{-8} mbar. Core level spectra were deconvoluted by using Voigt functions and linear background subtraction.

Intensity ratios $\frac{I_A}{I_B}$ were determined by evaluation of the integrals I_A and I_B of signal A and B, respectively. The error of the intensity ratio, $\Delta\left(\frac{I_A}{I_B}\right)$, was calculated following the propagation of errors:

$$\Delta\left(\frac{I_A}{I_B}\right) = \sqrt{\left(\frac{\partial\left(\frac{I_A}{I_B}\right)}{\partial I_A}\cdot\Delta I_A\right)^2 + \left(\frac{\partial\left(\frac{I_A}{I_B}\right)}{\partial I_B}\cdot\Delta I_B\right)^2}$$

Rewriting this equation reveals the relative error of the intensity ratio $\Delta\left(\frac{I_A}{I_B}\right)/\left(\frac{I_A}{I_B}\right)$:

$$\frac{\Delta\left(\frac{I_A}{I_B}\right)}{\frac{I_A}{I_B}} = \sqrt{\left(\frac{\Delta I_A}{I_A}\right)^2 + \left(\frac{\Delta I_B}{I_B}\right)^2}$$

Considering the error arising from the deconvolution of the core level spectra, we estimated a maximum relative error of each integral as follows:

$$\frac{\Delta I_A}{I_A} = \frac{\Delta I_B}{I_B} = 4\%$$

Hence, the relative error of an intensity ratio $\Delta\left(\frac{I_A}{I_B}\right)/\left(\frac{I_A}{I_B}\right)$ is approximately 6%.

3.4. Fourier-transform infrared spectroscopy (FTIR)

Infrared (IR) spectra were recorded on a PerkinElmer Frontier FT-IR spectrometer (PerkinElmer, Inc., Waltham, USA) by attenuated total reflection (ATR) technique. The signals are given in $\tilde{v}$ [cm^{-1}]. The second derivative of the transmission was obtained numerically after a five-point, two-degree polynomial function [40]. In order to achieve a better signal to noise ratio the derivative spectra were smoothed with an 11-point, two-degree polynomial Savitzky-Golay function following a procedure described by Seabourn et al. (2008) [41,42]. The secondary structures of gluten could then be analyzed in the amide III region [42–44] and the wavelength values characteristic for the discussed secondary structures were adopted from Seabourn et al. (2008) [42].

3.5. Rheological behavior

Rheological measurements of hydrated vital gluten were performed with a MCR 502 rheometer equipped with a CTD 180 chamber (Anton Paar GmbH, Graz, Austria) with a parallel plate-plate system (riffled steel plates PP25/P2) and a constant gap of 2 mm. After the sample was placed between the plates and excess material was removed, the sample surface still exposed to air was covered with paraffin oil to prevent dehydration and the sample was relaxed for 20 min. Measurements were performed at a frequency of 1 Hz and a shear deformation γ of 0.1% while heating from 20 to 95 °C at a heating rate of 0.5 °C/min. The loss factor tan(δ) was determined from the elastic modulus G′ and the viscous modulus G″. To calculate the inflection points of the loss factor as a function of the temperature, the roots of the second derivative of the loss factor after second order polynomial 20-point smoothing was used. All tests were performed in triplicate with a new sample preparation for every measurement.

3.6. Gluten protein extraction and RP-HPLC

Gluten proteins (gliadins and glutenins) were extracted based on a modified Osborne fractionation and determined by analytical RP-HPLC [45]. Vital gluten (20 mg) with added glass beads was extracted with 60% (v/v) ethanol (3 × 1.5 ml) to obtain the gliadins. Subsequently,

the residue was extracted with a glutenin extraction solution containing 50% (v/v) 1-propanol, 0.05 mol/l Tris-HCl (pH 7.5), 2 mol/l urea (w/v), 1% (w/v) dithiothreitol (DTT) (3 × 1.5 ml, 60 °C and under nitrogen atmosphere) to solubilize the glutenins. The extraction was performed by vortex mixing for 2 min, then magnetic stirring for 10 min at 20–22 °C (gliadins), respectively 30 min at 60 °C (glutenins), followed by centrifugation for 25 min at 3550 ×g at 20–22 °C. Corresponding extracts were collected and made up to a volume of 5.0 ml with the appropriate extraction solvent. All extractions were performed in triplicate. A Hitachi Merck instrument (VWR, Darmstadt, Germany) with a Dionex Acclaim™ 300 C18 column (3 μm, 30 nm, 2.1 × 150 mm, Thermo Fisher Scientific, Braunschweig, Germany) and the LaChrom Elite software were used to analyze the fractions. The following parameters were set: flow rate; 0.3 ml/min, column temperature; 60 °C, UV detection; 210 nm, injection volume; 20 μl, elution solvents; water/trifluoroacetic acid (TFA) (999/1, v/v) (A) and acetonitrile/TFA (999/1, v/v) (B). The solvent gradient was 0 min; 24% B, 20 min; 56% B, 21 min; 90% B, 26 min; 90% B, 27 min; 24% B, 37 min; 24% B. Peak integration and calculation of protein contents was based on a calibration with Prolamin Working Group (PWG)-gliadin (11.6 to 46.6 μg, dissolved in 60% (v/v)) [46]. The measured peak areas for gliadin and glutenin were put into relation to calculate a ratio of gliadin to total protein content.

3.7. Analysis and statistical evaluation

Peak identification of the rheological data was conducted with Matlab R2019a (The MathWorks, Inc., Natick, Massachusetts, USA). Evaluation of XPS data and TGA-MS data were done with IGOR Pro 6.37 (WaveMetrics, Oregon, USA). All further statistical evaluation was conducted with Origin 2017.

4. Results and discussion

4.1. Structural changes of dry gluten at high temperatures

The thermal effect on dry gluten was elaborated to characterize protein modification at high temperatures. As all vital gluten samples showed matching results only the spectra of the vital gluten sample C is shown exemplarily for all samples. Thermalgravimetric analysis (TGA) of vital gluten powder sample C shown in Fig. 1 and the combination with quadrupole mass spectrometry (QMS) in Fig. 2 outline distinct mass losses, starting with an initial degassing of H_2O at 100 °C.

The TGA curve stabilizes at 170 °C before decreasing again with the highest loss rate at 300 °C: This can be related to the formation of water bound within the material, carbon dioxide as well as volatile hydrocarbon species derived from QMS data shown in Fig. 2 (signals at mass-to-charge ratio (m/z) 13, 18 and 44 corresponding to CH^+, H_2O^+ and CO_2^+, respectively). In this range, dehydration as well as decarboxylation processes occur indicating progressive denaturation of the protein structures. This temperature range is in good agreement with the literature [47,48]. Above 500 °C, the carbon-based molecules are increasingly oxidized to almost complete conversion into gaseous products at 1000 °C.

To track changes of the surface composition and present functional groups up to ~3 nm in depth, samples were analyzed as are and after annealing at 70, 85, 170 and 250 °C in air for 2 h by XPS. The measurements were done for lower temperatures where denaturation should only take place in hydrated form and higher temperatures at which the TGA-MS curves showed clear indications for a compositional change in the dry material (Fig. 3). To characterize the material, high resolution spectra of the C 1s, O 1s and N 1s core levels were acquired. Note that we refrained from calculating absolute values for the elemental surface composition and compared peak areas ratios of different core levels instead. As all signals appear at different kinetic energies they bear a slightly different depth sensitivity. Calculating the surface composition demands an elemental distribution as a function of the distance from
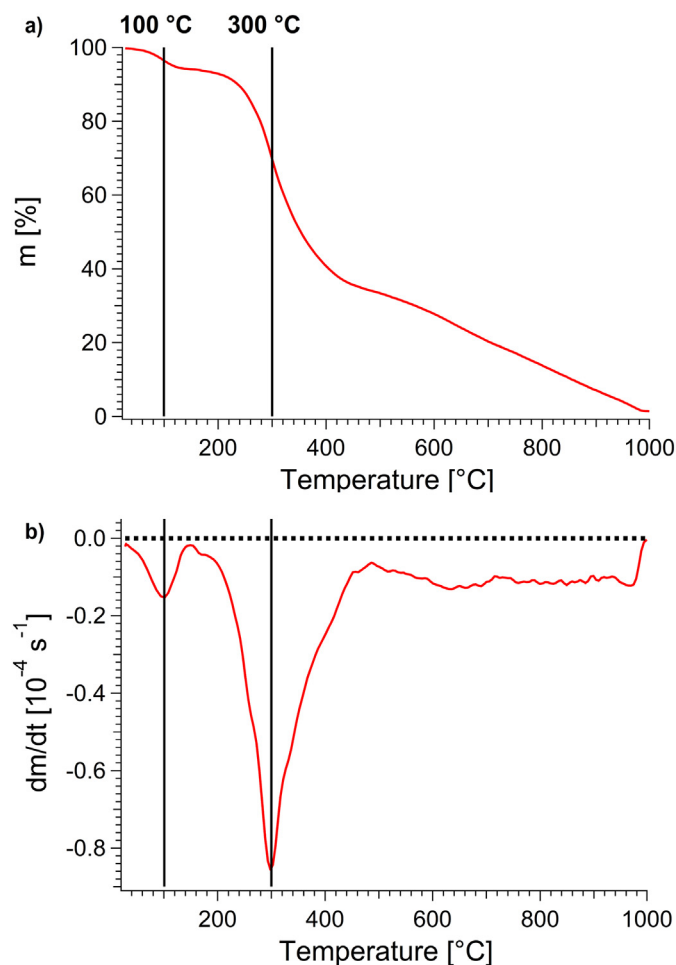
a)

b)

Fig. 1. (a) TGA curve of dry vital gluten sample C shows the mass loss as function of temperature and (b) its first derivative as a function of the mass loss rate. The mass of sample C decreases significantly around 100 °C as well as 300 °C.
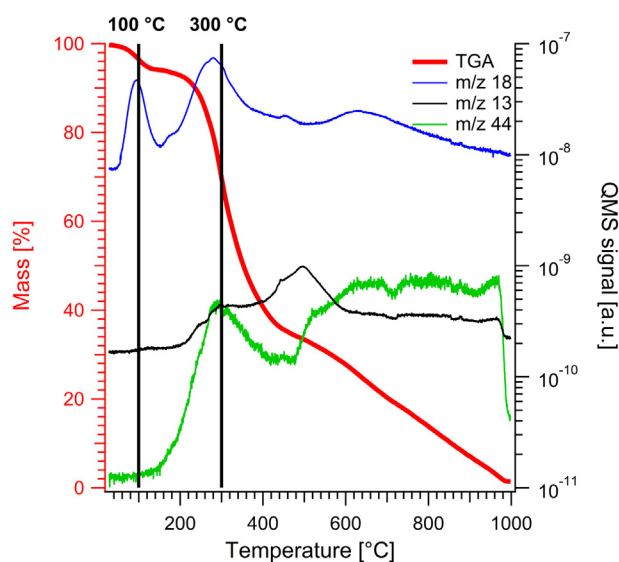

Fig. 2. Quadrupole mass spectrometry (QMS) of the gas phase emerging during the TGA experiment with vital gluten sample C. The signals of m/z 18, 13 and 44, corresponding to H_2O^+, CH^+ and CO_2^+, respectively, are shown together with the mass loss as a function of temperature.

the surface which remains unknown for complex protein structures. Hence, a peak area ratio was used which reflects both, the atomic ratio and the distribution with respect to the sample surface. The latter is influenced by changes in the protein folding.

No definable changes are visible at lower temperatures: Similar O 1s/C 1s and N 1s/C 1s ratios are found for all samples within a narrow range of ±10%. The relative signal intensities for C 1s, O 1s and N 1s of sample C reveal a lower N/C ratio at the protein surface after annealing to 170 °C while the O/C ratio remains constant within the error bars. A release of water from the sample at those temperatures observed by TGA-MS cannot be seen in XPS. The absence of this effect might be attributed to the ultrahigh vacuum conditions during the XPS measurement that can also lead to water evaporation from a protein sample even at room temperature. The decrease of the N/C ratio might indicate a change in the protein structure as no significant amount of N-related species, e.g. ammonia or dinitrogen, was detected by TGA-MS. Hence, a reduction of amino groups exposed to the surface due to a change of the protein folding is plausible [49]. Another hint for a changed protein folding is the increase of the N/C ratio at 250 °C exceeding the initial level. The simultaneous drop of the O 1s/C 1s intensity ratio most probably relies on decarboxylation processes upon thermal degradation already discussed in the TGA-MS section. Hence, an elevated protein denaturation is detected at 250 °C.

The temperature-dependent decomposition of the material can also be followed by deconvoluting the C 1s core level, depicted in Fig. 4, showing the chemical environment of the carbon-related species at different temperatures. Three different species can be derived from the peak shape which can be attributed by comparing their binding energy to literature values: sp^3- and sp^2-C at 284.5 eV, C—N and C—O species at 287 eV as well as carbonyl species at ca. 288 eV [50]. At 170 °C, the fraction of C=O species slightly increases at the expense of C—C species. At 250 °C the opposite trend for the C—C species can be seen as the fraction increases a lot while the amount of C—O and C—N species decreases significantly. This indicates a change in protein conformation due to thermal denaturation processes prior to a complete compositional change at 250 °C, where denaturation can be explained by the loss of C—O species, like CO_2 (see also Fig. 2).

The functional groups of the protein and the spatial protein structure was studied by FTIR to compare with the findings of the XPS measurements. Fig. 5 shows a shift of the bands characterizing the secondary structures of gluten upon annealing at high temperatures [42]. This indicates a different protein folding and, thus, implicates a structural change in the sample. At 170 °C (orange), a shift of the β-sheet signal at 1242 cm^{-1} could be related to an exposure of N-related species due to a changed protein folding (see Fig. 3). Heating at 170 °C does not (entirely) destroy secondary structures and/or degrades material around the α -helices and β -sheets. At 250 °C (red), the IR-signal shows a completely different course for α-helix (1317 cm^{-1}), β-turn (1285 cm^{-1}) and β-sheet (1242 cm^{-1}) related structures indicating that the protein has entirely changed its properties and loses its functionality as a protein.

TGA-MS, XPS and FTIR measurements indicate a structural change of the proteins at 170 °C, which can be linked to the desorption of water as well as to altered secondary structure elements. Elevated denaturation processes including vast structural changes and chemical decomposition processes, e.g. water formation and decarbonylation, occur at 250 °C. This means a complete loss of protein functionality. Protein folding up to denaturation and destruction of dry gluten samples can therefore be observed by XPS, TGA-MS and FITR.

While the analysis of dry gluten is important to see thermal effects on the protein for example during milling processes, a different denaturation pattern is expected for hydrated gluten. As Gontard and Ring (1996) aptly describe, the addition of water acting as a plasticizer with low molecular weight increases the mobility of a polymer by adding free volume to the system [51]. Therefore, the hydration of gluten in theory has the same effect on the molecular mobility as increasing
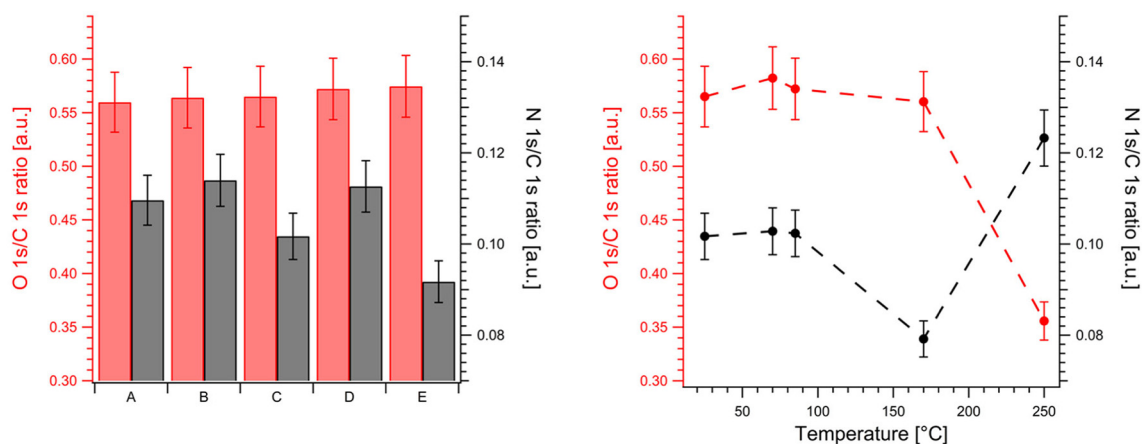
Fig. 3. O 1s/C 1s ratio (red) and N 1s/C 1s ratio (black) of all dry vital gluten samples A-E as are (left). The figure on the right shows exemplarily the composition of sample C after annealing to different temperatures in air. Changes in the surface composition prove denaturation of protein structures by different protein folding and loss of functional groups at 170 °C.

the temperature. In literature, thermal effects on the polymer described with T_g verified a much higher transition temperature for dry samples, where less mobility is available [12,14,15] and thermal diffusivity decreases [52]. In the following chapter thermal effects on hydrated gluten are observed with an additional focus on the compositional differences of the samples.

4.2. Structural changes of hydrated gluten at thermal denaturation

During the formation of edible and non-edible products, hydrated gluten is exposed to thermal stress. Therefore, the structural development of the hydrated gluten network was investigated with an oscillatory sweep during a temperature ramp. The network functionality depending on the temperature increase was investigated on samples with different fractions of gliadin to total protein mass (gliadin and glutenin). Fig. 6 presents the loss factor tan (δ) at different temperatures (20 to 95 °C); the loss factor tan (δ) serves as a measure for the viscous modulus G˝ in proportion to the elastic modulus G´.

Two inflection points of the decreasing loss factor occur during the heating; the first one in a broad range of 56.14 ± 0.63 °C to 63.70 ±

1.09 °C (T_1 range), the second one in a smaller range of 78.86 ± 0.01 °C to 81.36 ± 1.27 °C (T_2 range). These points mark the temperatures at which structural alteration occurs as the ratio of elastic to viscous modulus changes. As depicted in Fig. 7, the T_1 range can be linked to the ratio of gliadin to total protein mass of the samples, which was calculated from RP-HPLC measurements (see supplementary material). The different gliadin and glutenin contents in the samples only show an effect on the gluten functionality when heating the sample. Sample A with the lowest gliadin fraction (59.3%) undergoes a first structural change at 56.14 ± 0.63 °C while sample E with the highest gliadin fraction of 63.7% shows the same effect at 63.70 ± 1.09 °C. Sample A significantly differs from sample E for T_1 at a significance level of 0.05, while for T_2 there are no significant differences between the samples. As gliadin contributes to the viscous factors of a sample [22], the temperature, at which a rheological change can be detected is higher, the more gliadin is in the sample [53]. Gliadin appears to be unaltered and more temperature-stable than glutenin, which was also found by Schofield et al. (1983) using chromatography methods [53]. The lipid content does not show any influence on the viscoelastic properties of gluten [54], which is approved by own data (see Table
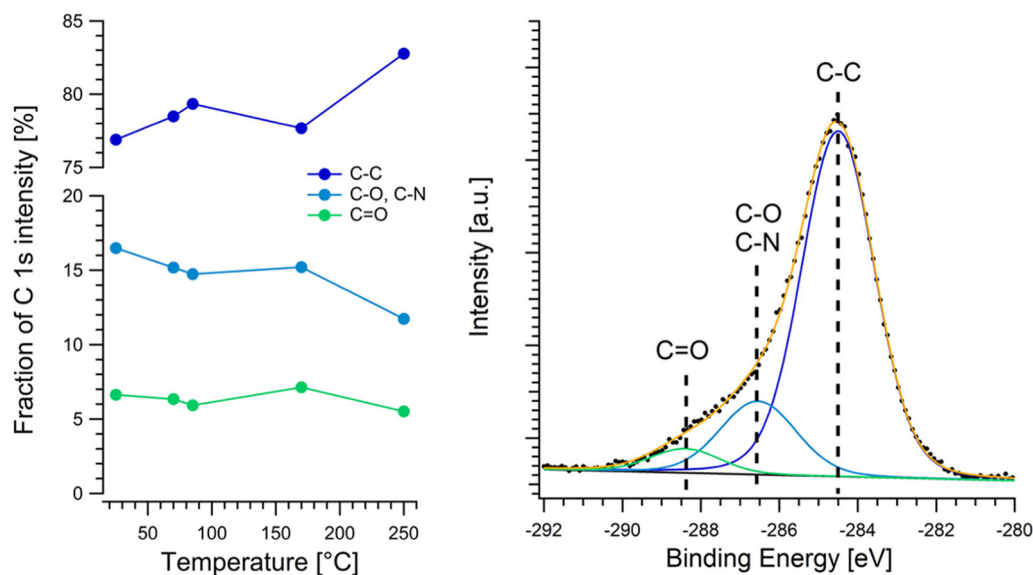

Fig. 4. Change of carbon-related surface species of vital gluten sample C. Left: Fractions of C 1s components depending on the heat treatment show a large increase of C—C species at 250 °C at the expense of C—O and C—N species indicating protein denaturation. Right: Deconvoluted C 1s signal showing C—C, C—O, C—N and C=O bindings at their specific binding energy [50].
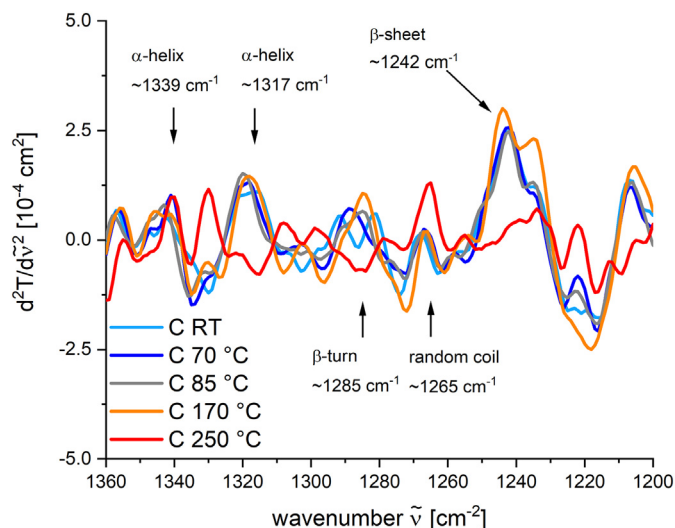
Fig. 5. Second derivative of the FTIR spectra of vital gluten sample C as is and after heating to 70, 85, 170 and 250 °C. A slight increase in the β-sheet related band occurs at 170 °C before a total change of all signals is found at 250 °C.

Fig. 7. Transition temperatures T_1 and T_2 at which an inflection point of the loss factor tan (δ) of hydrated gluten samples (A-E) as a function of the gliadin content (with respect to the total protein mass) can be seen. The slope and its error was extracted by linear regression in x direction.

1). The starch content of the samples is in a range, where no significant contribution to the rheological behavior is assumed.

Besides the T_g of the protein [19], the gliadin/glutenin ratio also influences the equilibrium of elasticity and viscosity in the network [6,22] and the gliadin/glutenin fraction has been described as a contributing factor to rheological effects [55–57]. Irreversible changes in both T ranges may occur. According to literature, the polymer size distribution is affected through sulfhydryl-disulfide (SH-SS) exchange reactions [7,57] and intramolecuar SS bonds tend to transform into intermolecular SS- and non-SS bonds as assumed by Rombouts et al. (2011) [47] in the course of polymerization.

The impact of the described two-step denaturation is not only visible in the pure protein, but a clear effect can also be seen when the material is incorporated in a system such as dough [58]. It can be assumed that the incorporation of gluten in any system will show network effects at the above-mentioned temperature ranges. Regarding non-food products the shift towards a more elastic and less viscous polymer can be
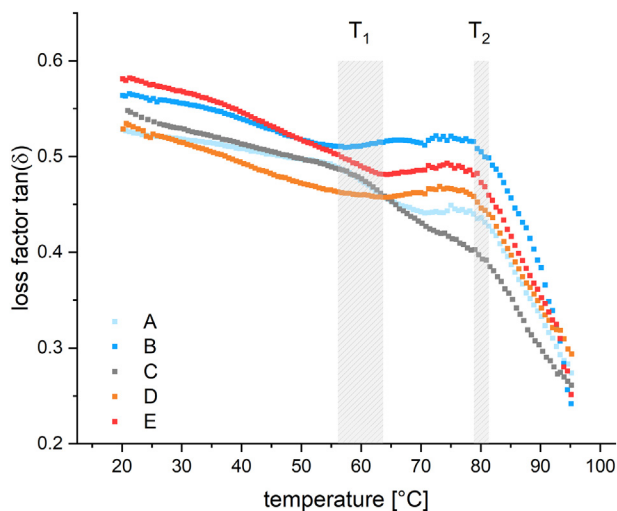
used as an advantage when the material needs to stay in shape and still be flexible despite physical stresses.

To further characterize the structural alterations of the thermoset protein indicated by the above-mentioned rheological effects, FTIR measurements of wet hydrated gluten samples at room temperature and after heating above T_1 at 70 °C and above T_2 at 85 °C were performed (see Fig. 8). A shift of the α-helix bands (1339 cm^{-1} and 1317 cm^{-1}) is observed when heating above 70 °C, indicating that a partial denaturation takes place. Heating up to 85 °C causes an additional change of the signal for the β-turns. The IR spectra therefore confirm the two-step denaturation characteristics of hydrated gluten observed in the rheological measurements at two temperature ranges. For gliadins, Georget et al. (2006) suggested a loss of α-helical structures upon heating to only 45 °C, while there is a formation of new β-structures when heating to 55 °C [25].

5. Conclusion

The structural changes and thermal denaturation of different gluten macropolymers, were followed using spectroscopic and rheological methods. The same gluten samples were analyzed in both, dry and

Fig. 6. Hydrated vital wheat gluten samples A-E heated from 20 to 95 ¬C in an oscillatory sweep show a decreasing loss factor with two inflection points. The first inflection point occurs at 56.14 ± 0.63 °C to 63.70 ± 1.09 °C, the second one at 78.86 ± 0.00 °C to 81.36 ± 1.27 °C and they imply a structural change in the sample.
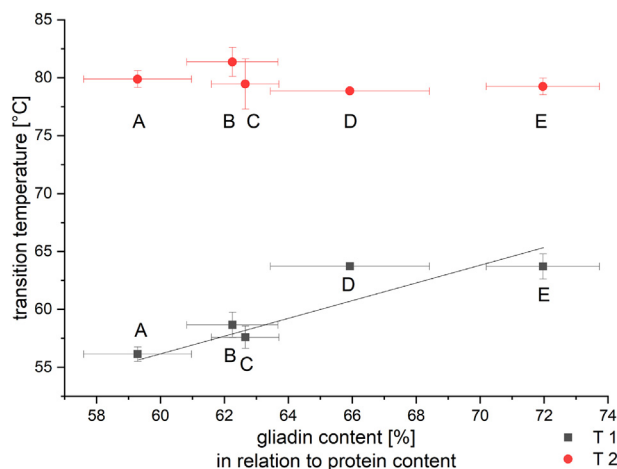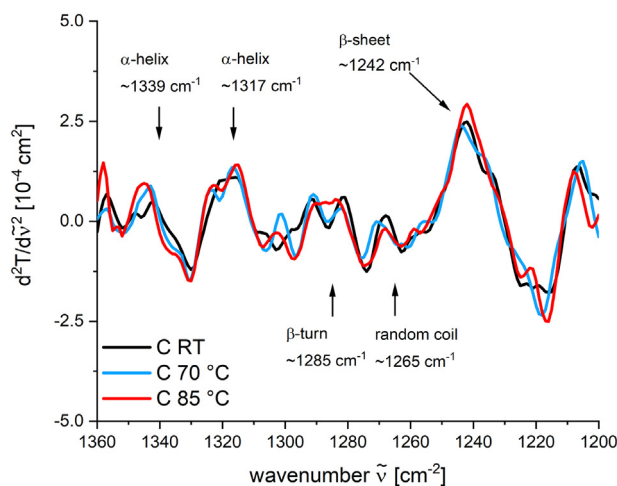

Fig. 8. Second derivative of the processed FTIR spectra of the hydrated sample C at room temperature and after annealing at 70 °C and 85 °C for 5 h in a hermetically sealed tube.

hydrated state, to describe the range of thermally induced changes the thermosetting protein can undergo. As the molecular mobility and diffusivity of a protein increases with the water content [51,52], thermal effects on hydrated gluten appear at much lower temperatures than on dry vital gluten. Gliadin to total protein ratio correlated with the temperature at which a first rheological effect was seen, implicating protein denaturation. Vibrational spectroscopy confirms that the polymer denatures in two temperature ranges by showing shifts of the α-helices bands after a first heating step at 70 °C and an additional change of the β-turn bands after heating at 85 °C proving alteration of the protein folding and, thus, a stepwise denaturation. Upon denaturation of the hydrated gluten protein will achieve resilient, elastic and flexible properties that are a requirement for a sustainable and biodegradable substitute for plastic products such as foils and nets.

A much higher temperature stability is expressed by dry vital gluten. It is the first time that the course of dry gluten protein denaturation was correlated with the change of the chemical composition by assessing the elementary surface composition and the chemical environment (XPS), the secondary structures (FTIR) as well as the gaseous products evolving during thermal decomposition (TGA-MS). After a distinct mass loss due to residual water, the gluten mass stabilizes at 170 °C, before reaching the highest loss rate at 250 °C, where water, carbon dioxide and volatile hydrocarbon species are formed. Decarboxylation and dehydration processes indicate the progressive denaturation of protein. The change in protein structure and decarboxylation processes are also observed by XPS as reversible and irreversible changes in the surface composition upon heating. This implicated structural change of the protein is confirmed by FTIR. Besides a shift of the β-sheet signal at 170 °C, the protein appears to have most of the secondary structures still in intact condition. At 250 °C, the IR signal shows an entirely different course indicating complete loss of protein functionality. When rehydrating structurally altered gluten, the development of inter- and intramolecular connections will be less and depending on the degree of denaturation might completely lose the ability to form a consistent network. This will make the material more soluble and shapeable or even act as a thickener. In combination with other biopolymers this can be a promising starting point for the development of biodegradable materials.

The connection between structural and mechanical response to heat exposure for gluten in both, dry and hydrated state, gives a first insight on how the protein folding impacts network properties. Knowing the dynamics of protein denaturation makes the use and processing of this polymer more predictable, which is very valuable for processing the material in combination with other polymers. Depending on the hydration of the protein, the material characteristics is very versatile and by knowing more about the procedure of protein denaturation a step towards customizing the polymer can be made.

Acknowledgements

Author statement

All persons who meet authorship criteria are listed as authors, and all authors certify that they have participated sufficiently in the work to take public responsibility for the content, including participation in the concept, design, analysis, writing, or revision of the manuscript. Furthermore, each author certifies that this material or similar material has not been and will not be submitted to or published in any other publication.

CRediT authorship contribution statement

Monika C. Wehrli: Conceptualization (lead); Methodology (lead); Software (equal); Validation (lead); Formal analysis (equal); Investigation (equal); Data curation (equal); Visualization (lead); Project administration (lead); Writing – Original Draft Preparation (lead); Writing - Review & Editing (equal).

Tim Kratky: Conceptualization (support); Methodology (support); Software (equal); Validation (support); Formal analysis (equal); Investigation (equal); Data curation (equal); Visualization (support); Writing – Original Draft Preparation (support); Writing - Review & Editing (equal).

Marina Schopf: Investigation (equal); Writing - Review & Editing (support).

Katharina A. Scherf: Resources (equal); Funding acquisition (equal); Writing - Review & Editing (support).

Thomas Becker: Resources (equal); Funding acquisition (equal); Project administration (support); Supervision (equal); Writing - Review & Editing (support).

Mario Jekle: Conceptualization (support); Resources (equal); Funding acquisition (equal); Project administration (support); Supervision (lead); Writing – Review & Editing (equal).

Declaration of competing interest

None.

Appendix A. Supplementary data

Supplementary data to this article can be found online at https://doi.org/10.1016/j.ijbiomac.2021.01.008.

References

[1] S.W. Cho, M. Gällstedt, E. Johansson, M.S. Hedenqvist, Injection-molded nanocomposites and materials based on wheat gluten, Int. J. Biol. Macromol. 48 (1) (2011) 146–152.

[2] L. Day, M.A. Augustin, I.L. Batey, C.W. Wrigley, Wheat-gluten uses and industry needs, Trends Food Sci. Technol. 17 (2006) 82–90.

[3] F. Ortolan, C.J. Steel, Protein characteristics that affect the quality of vital wheat gluten to be used in baking: a review, Compr. Rev. Food Sci. Food Saf. 16 (3) (2017) 369–381.

[4] P.L. Weegels, R.J. Hamer, J.D. Schofield, Functional properties of wheat glutenin, J. Cereal Sci. 23 (1) (1996) 1–17.

[5] P.W. Gras, R.S. Anderssen, M. Keentok, F. Bekes, R. Appels, Gluten protein functionality in wheat flour processing: a review, Aust. J. Agric. Res. (January) (2001).

[6] N. Ooms, J.A. Delcour, How to impact gluten protein network formation during wheat flour dough making, Curr. Opin. Food Sci. 25 (2019) 88–97.

[7] W.S. Veraverbeke, J.A. Delcour, Wheat protein composition and properties of wheat glutenin in relation to breadmaking functionality wheat protein composition and properties of wheat glutenin in relation to breadmaking functionality, Crit. Rev. Food Sci. Nutr. 42 (3) (2002) 179–208.

[8] K.Q. Wang, S.Z. Luo, X.Y. Zhong, J. Cai, S.T. Jiang, Z. Zheng, Changes in chemical interactions and protein conformation during heat-induced wheat gluten gel formation, Food Chem. 214 (2017) 393–399.

[9] I. Rombouts, B. Lagrain, J.A. Delcour, Heat-induced cross-linking and degradation of wheat gluten, serum albumin, and mixtures thereof, J. Agric. Food Chem. 60 (40) (2012) 10133–10140.

[10] N. Guerrieri, E. Alberti, V. Lavelli, P. Cerletti, Use of spectroscopic and fluorescence techniques to assess heat-induced molecular modifications of gluten, Cereal Chem. 73 (3) (1996) 368–374.

[11] R. Bale, H.G. Muller, Application of the statistical theory of rubber elasticity to the effect of heat on wheat gluten, J. Food Technol. 5 (1970) 295–300.

[12] H.J. Kersting, W. Kempf, DSC investigations on vital gluten, Starch - Stärke 43 (1) (1991) 32–34.

[13] Y.I. Matveev, V.Y. Grinberg, I.V. Sochava, V.B. Tolstoguzov, Glass transition temperature of proteins. Calculation based on the additive contribution method and experimental data, Food Hydrocoll. 11 (2) (1997) 125–133.

[14] A. Leon, C.M. Rosell, C.B. De Barber, A differential scanning calorimetry study of wheat proteins, Eur. Food Res. Technol. 217 (1) (2003) 13–16.

[15] R.C. Hoseney, K.J. Zeleznak, C.S. Lai, Wheat gluten: a glassy polymer - communication to the editor, Am. Assoc. Cereal Chem. 63 (3) (1986) 285–286.

[16] H. Wieser, Chemistry of gluten proteins, Food Microbiol. 24 (2) (2007) 115–119.

[17] P. Shewry, A.S. Tatham, J. Forde, M. Kreis, B.J. Miflin, The classification and nomenclature of wheat gluten proteins: a reassessment, J. Cereal Sci. 4 (1986) 97–106.

[18] H. Goesaert, K. Brijs, W. S. Veraverbeke, C. M. Courtin, K. Gebruers, and J. A. Delcour, "Wheat flour constituents: how they impact bread quality, and how to impact their functionality," Trends Food Sci. Technol.

[19] B.S. Khatkar, S. Barak, D. Mudgil, Effects of gliadin addition on the rheological , microscopic and thermal characteristics of wheat gluten, Int. J. Biol. Macromol. 53 (2013) 38–41.

[20] M.T. Kalichevsky, E.M. Jaroszkiewicz, J.M.V. Blanshard, Glass transition of gluten. 1: gluten and gluten—sugar mixtures, Int. J. Biol. Macromol. 14 (5) (1992) 257–266 Oct.

[21] M.T. Kalichevsky, E.M. Jaroszkiewicz, J.M.V. Blanshard, Glass transition of gluten. 2: the effect of lipids and emulsifiers, Int. J. Biol. Macromol. 14 (5) (1992) 267–273.

[22] P.R. Shewry, A.S. Tatham, F. Barro, P. Barcelo, P. Lazzeri, Biotechnology of breadmaking: unraveling and manipulating the multi-protein gluten complex, Bio/Technology 13 (11) (1995) 1185–1190.

[23] P.L. Weegels, J.A. Verhoek, A.M.G. de Groot, R.J. Hamer, Effects on gluten of heating at different moisture contents. I. Changes in functional properties, J. Cereal Sci. 19 (1994) 31–38.

[24] P.L. Weegels, A.M.G. de Groot, J.A. Verhoek, R.J. Hamer, Effects on gluten of heating at different moisture contents. II. Changes in physico-chemical properties and secondary structure, J. Cereal Sci. 19 (1994) 39–47.

[25] D.M.R. Georget, P.S. Belton, Effects of temperature and water content on the secondary structure of wheat gluten studied by FTIR spectroscopy, Biomacromolecules 7 (2) (2006) 469–475.

[26] P.S. Belton, A. Colquhoun, A. Grant, N. Wellner, FTIR and NMR studies on the hydration of a high-Mr subunit of gluten, Int. J. Biol. Macromol. 17 (2) (1995) 437–441.

[27] A. Almutawah, S.A. Barker, P.S. Belton, Hydration of gluten: a dielectric, calorimetric, and fourier transform infrared study, Biomacromolecules 8 (5) (2007) 1601–1606.

[28] V. Kontogiorgos, Microstructure of hydrated gluten network, Food Res. Int. 44 (9) (2011) 2582–2586.

[29] N. Wellner, et al., Changes in protein secondary structure during gluten deformation studied by dynamic fourier transform infrared spectroscopy, Biomacromolecules 6 (1) (2005) 255–261.

[30] F. Rasheed, et al., Macromolecular changes and nano-structural arrangements in gliadin and glutenin films upon chemical modification - relation to functionality, Int. J. Biol. Macromol. 79 (2015) 151–159.

[31] J.F. Watts, J. Wolstenholme, Applications of electron spectroscopy in materials science, An Introduction to Surface Analysis by XPS and AES, vol. 3, , 2003.

[32] J. Ertl, X-Ray Photoelectron Spectroscopy (XPS), 1966.

[33] M.I.P. Kovacs, B.X. Fu, S.M. Woods, K. Khan, Thermal stability of wheat gluten protein : its effect on dough properties and noodle texture, J. Cereal Sci. 39 (2004) 9–19.

[34] F. Rasheed, T.S. Plivelic, R. Kuktaite, M.S. Hedenqvist, E. Johansson, Unraveling the structural puzzle of the giant glutenin polymer - an interplay between protein polymerization, nanomorphology, and functional properties in bioplastic films, ACS Omega 3 (5) (2018) 5584–5592.

[35] A. Mohamed, V.L. Finkenstadt, S.H. Gordon, G. Biresaw, D.E. Palmquist, P. Rayas-Duarte, Thermal properties of PLC/gluten bioblends characterized by TGA, DSC, SEM and infrared-PAS, J. Appl. Polym. Sci. 110 (2008) 3256–3266.

[36] L.S. Zárate-Ramírez, I. Martínez, A. Romero, P. Partal, A. Guerrero, Wheat gluten-based materials plasticised with glycerol and water by thermoplastic mixing and thermomoulding, J. Sci. Food Agric. 91 (4) (2011) 625–633.

[37] A. Mohamed, S.H. Gordon, C.J. Carriere, S. Kim, Thermal characteristics of polylactic acid/wheat gluten blends, J. Food Qual. 29 (2006) 266–281.

[38] G. Neill, A.H. Al-Muhtaseb, T.R.A. Magee, Optimisation of time/temperature treatment, for heat treated soft wheat flour, J. Food Eng. 113 (3) (2012) 422–426.

[39] S. Brandner, T. Becker, M. Jekle, Wheat dough imitating artificial dough system based on hydrocolloids and glass beads, J. Food Eng. 223 (2017) 144–151.

[40] H. Susi, D.M. Byler, Protein structure by Fourier transform infrared spectroscopy: second derivative spectra, Biochem. Biophys. Res. Commun. 115 (1) (1983) 391–397.

[41] A. Savitzky, M.J.E. Golay, Smoothing and differentiation of data by simplified least squares procedures, Anal. Chem. 36 (8) (1964) 1627–1639.

[42] B.W. Seabourn, O.K. Chung, P.A. Seib, P.R. Mathewson, Determination of secondary structural changes in gluten proteins during mixing using fourier transform horizontal attenuated total reflectance spectroscopy, J. Agric. Food Chem. 56 (11) (2008) 4236–4243.

[43] S. Cai, B.R. Singh, Identification of β-turn and random coil amide III infrared bands for secondary structure estimation of proteins, Biophys. Chem. 80 (1999) 7–20.

[44] S. Cai, B.R. Singh, A distinct utility of the amide III infrared band for secondary structure estimation of aqueous protein solutions using partial least squares methods, Biochemistry 43 (2004) 2541–2549.

[45] M. Schopf and K. A. Scherf, "Wheat cultivar and species influence variability of gluten ELISA analyses based on polyclonal and monoclonal antibodies R5 and G12," J. Cereal Sci., vol. 83, no. May, pp. 32–41, 2018.

[46] R. van Eckert, E. Berghofer, P.J. Ciclitira, F. Chirdo, S. Denery-papini, H.J. Ellis, Towards a New Gliadin Reference Material – Isolation and Characterisation, vol. 43, 2006 331–341.

[47] X. Wang, L. Sheng, X. Yang, Pyrolysis characteristics and pathways of protein, lipid and carbohydrate isolated from microalgae Nannochloropsis sp, Bioresour. Technol. 229 (2017) 119–125.

[48] S. Wang, Y. Hu, Z. He, Q. Wang, S. Xu, Study of pyrolytic mechanisms of seaweed based on different components (soluble polysaccharides, proteins, and ash), J. Renew. Sustain. Energy 9 (2) (2017).

[49] I. Rombouts, B. Lagrain, M. Brunnbauer, P. Koehler, K. Brijs, J.A. Delcour, Identification of isopeptide bonds in heat-treated wheat gluten peptides, J. Agric. Food Chem. 59 (4) (2011) 1236–1243.

[50] T. Kuila, S. Bose, A.K. Mishra, P. Khanra, N.H. Kim, J.H. Lee, Chemical functionalization of graphene and its applications, Prog. Mater. Sci. 57 (7) (2012) 1061–1105.

[51] N. Gontard, S. Ring, Edible wheat gluten film: influence of water content on glass transition temperature, J. Agric. Food Chem. 44 (11) (1996) 3474–3478.

[52] T.D. Strecker, R.P. Cavalieri, Y. Pomeranz, Wheat Gluten and Glutenin Thermal Conductivity and Diffusivity at Extruder Temperatures, vol. 59, 1994 1244–1246 no. 6.

[53] J.D. Schofield, R.C. Bottomley, M.F. Timms, M.R. Booth, The effect of heat on wheat gluten and the involvement of sulphydryl-disulphide interchange reactions, J. Cereal Sci. 1 (4) (1983) 241–253.

[54] J. Hargreaves, Y. Popineau, D. Marion, J. Lefebvre, M. Le Meste, Gluten viscoelasticity is not lipid-mediated. A rheological and molecular flexibility study on lipid and non-prolamin protein depleted glutens, J. Agric. Food Chem. 43 (5) (1995) 1170–1176.

[55] S. Barak, D. Mudgil, B.S. Khatkar, Relationship of gliadin and glutenin proteins with dough rheology, flour pasting and bread making performance of wheat varieties, LWT Food Sci. Technol. 51 (1) (2013) 211–217.

[56] M. Cornec, Y. Popineau, J. Lefebvre, Characterisation of gluten subfractions by SE-HPLC and dynamic rheological analysis in shear, J. Cereal Sci. 19 (1994) 131–139.

[57] J. Lefebvre, Y. Popineau, G. Deshayes, L. Lavenant, Temperature-induced changes in the dynamic rheological behavior and size distribution of polymeric proteins for glutens from wheat near-isogenic lines differing in HMW glutenin subunit composition, Cereal Chem. 77 (2) (2000) 193–201.

[58] A.E. Verbauwhede, et al., Microscopic investigation of the formation of a thermoset wheat gluten network in a model system relevant for bread making, Int. J. Food Sci. Technol. 55 (2) (2020) 891–898.